Thermal effects on nuclear matter properties

Lucas Tonetto[1,2,*] and Omar Benhar[2,1,†]

[1]*Dipartimento di Fisica, "Sapienza" University of Rome, Piazzale Aldo Moro, 5. 00185 Roma, Italy*
[2]*INFN, Sezione di Roma, Piazzale Aldo Moro, 5. 00185 Roma, Italy*

(Received 15 August 2022; accepted 2 November 2022; published 16 November 2022)

A quantitative description of the properties of hot nuclear matter will be needed for the interpretation of the available and forthcoming astrophysical data, providing information on the postmerger phase of a neutron star coalescence. We have employed a recently developed theoretical model, based on a phenomenological nuclear Hamiltonian including two- and three-nucleon potentials, to study the temperature dependence of average and single-particle properties of nuclear matter relevant to astrophysical applications. The possibility to represent the results of microscopic calculations using simple and yet physically motivated parametrizations of thermal effects, suitable for use in numerical simulations of astrophysical processes, is also discussed.

DOI: 10.1103/PhysRevD.106.103020

I. INTRODUCTION

Understanding the structure and dynamics of hot nuclear matter at the microscopic level is long known to be essential for the description of both supernovae and protoneutron stars [1–4]. More recently, thermal modifications of the equation of state (EOS) of neutron star matter have been also shown to play a critical role in the merger and postmerger phases of binary neutron star coalescence [5–9]. In this context, it has to be pointed out that an accurate description of finite-temperature effects is needed to study not only the equilibrium properties determining the density dependence of matter pressure, but also the occurrence of phenomena involving dissipation mechanisms, such as bulk viscosity [10] and neutrino emission [4,11–14].

The large dataset of zero-temperature EOSs available for use in simulations and data analysis—for a comprehensive catalog see Ref. [15]—is contrasted by a scarce number of EOSs of hot nuclear matter spanning the relevant regime, which is believed to extend to temperatures as high as 100 MeV [16,17].

The EOS of hot nuclear matter is often obtained using Skyrme-type effective interactions [18] or the relativistic mean field (RMF) approach [19]. More comprehensive studies of the properties of neutron star matter at nonzero temperature have been carried out within the framework of nuclear many-body theory, in which nuclear dynamics is described by a phenomenological Hamiltonian, strongly constrained by the observed properties of the two- and three-nucleon systems. Recent calculations along this line have been performed using both G-matrix perturbation theory [20] and the formalism of correlated basis functions [21].

A number of theoretical studies of the properties of hot nuclear matter have been also carried out using different many-body techniques and nuclear Hamiltonians obtained within the framework of chiral effective field theory (χEFT) [22–25]. It has to be pointed out, however, that the dynamical model based on χEFT is not expected to be applicable to the density region relevant to neutron stars [26,27].

The authors of Refs. [21,28] have developed a procedure to obtain from a phenomenological nuclear Hamiltonian a well-behaved effective potential, suitable to carry out perturbative calculations in the basis of eigenstates of the noninteracting system. This approach, in which the effects of irreducible three-nucleon interactions are consistently taken into account at microscopic level, allows to perform calculations of a variety of properties of dense nuclear matter with arbitrary proton fraction and temperatures in the region of $T \ll m_\pi$, $m_\pi \approx 150$ MeV being the mass of the π meson, in which thermal effects are not expected to significantly affect strong-interaction dynamics. Thermodynamic consistency is also achieved by construction, through a proper definition of the grand canonical potential [21].

The present work is primarily meant as a follow-up to the study of Benhar *et al.* [21], and provides a detailed analysis of the impact of thermal effects on specific properties of charge-neutral and β-stable matter relevant to neutron stars, such as the proton and neutron energy spectra and effective masses.

We will also examine the possibility of using simple approximated procedures to parametrize deviations from the zero-temperature EOS associated with thermal effects. The development of such procedures is of utmost importance, because their availability will enable to perform numerical simulations using EOSs based on a reliable treatment of the zero-temperature limit. Pinning down the validity and limitations of the proposed procedures,

*lucas.tonetto@uniroma1.it
†omar.benhar@roma1.infn.it

through a direct comparison with the predictions of fully microscopic calculations, will help to firmly establish their applicability.

A widely used, although admittedly oversimplified, parametrization is obtained from the so-called "hybrid-EOS" approach, in which thermal modifications of the thermodynamic functions of cold nuclear matter are approximated by the corresponding quantities of an ideal fluid [7,29–33].

Within this scheme, pressure and internal energy per nucleon are respectively written in the form

$$p = p_{\rm cold} + p_{\rm th},$$
$$e = e_{\rm cold} + e_{\rm th},$$

and the thermal contribution to the pressure at nucleon density ϱ and temperature T is parametrized by the adiabatic index, $\Gamma_{\rm th}$, according to

$$p_{\rm th}(\varrho, T) = \varrho\, e_{\rm th}(\Gamma_{\rm th} - 1). \tag{1}$$

The above procedure involves the drastic assumption that the adiabatic index be independent of both density and temperature. However, a comparison between the pressure obtained from Eq. (1) and that resulting from microscopic calculations based on advanced models of nuclear dynamics shows that $\Gamma_{\rm th}$ does, in fact, depend strongly on density, and that the dependence on temperature, while being weaker, is also non-negligible [7].

A more advanced parametrization, aimed at improving the description of the thermal pressure in the high-density region, has been recently proposed by Raithel *et al.* [16]. Within this approach, the prediction of the ideal fluid model—which is known to overestimate pressure at large densities—is replaced with that obtained from the leading term of the Sommerfeld expansion, which allows to systematically include degeneracy effects [34]. Microscopic nuclear dynamics is taken into account, using nucleon effective masses obtained from RMF models of nuclear matter.

To assess the accuracy and range of applicability of the simple and yet physically motivated parametrization of Ref. [16], we have compared its predictions to the results obtained from microscopic calculations of β-stable matter at temperatures up to 50 MeV, carried out within the formalism described in Ref. [21].

The manuscript is organized as follows. In Sec. II we outline the dynamical model underlying our theoretical approach, as well as the main elements of the formalism employed to study the properties of hot nuclear matter. Section III reports the results of a detailed analysis of thermal effects on both single-particle and average nuclear matter properties, while in Sec. IV we discuss a comparison with the results of Raithel *et al.* [16]. Finally, In Sec. V we summarize our findings and state the conclusions.

II. THEORETICAL MODEL

In this section, we summarize the main features of our theoretical model. We discuss both the underlying description of nuclear dynamics and the formalism employed to carry out calculations of the relevant properties of hot nuclear matter.

A. Nuclear dynamics

Nuclear many-body theory (NMBT) is based on the hypothesis that all nucleon systems—from the deuteron to neutron stars—can be described in terms of pointlike protons and neutrons, whose dynamics is dictated by the Hamiltonian

$$H = \sum_i \frac{p_i^2}{2m} + \sum_{i<j} v_{ij} + \sum_{i<j<k} V_{ijk}, \tag{2}$$

with m and $\mathbf{p}_i$ denoting mass and momentum of the ith particle.[1]

The nucleon-nucleon (NN) potential, usually written in the form

$$v_{ij} = \sum_p v^p(r_{ij}) O^p_{ij}, \tag{3}$$

where $r_{ij} = |\mathbf{r}_i - \mathbf{r}_j|$ is the distance between the interacting particles, is designed to reproduce the measured properties of the two-nucleon system, in both bound and scattering states, and reduces to the Yukawa one-pion exchange potential at large distances. The sum in Eq. (3) includes up to 18 terms, the corresponding operators, O^p, being needed to describe the strong spin-isospin dependence and noncentral nature of nuclear forces, as well as the occurrence spin-orbit interactions and small violations of charge symmetry and charge independence [35].

The addition of the three-nucleon (NNN) potential V_{ijk} is needed to take into account the effects of irreducible three-body interactions, reflecting the occurrence of processes involving the internal structure of the nucleons.

The results reported in this article have been obtained using an *effective interaction* derived from the phenomenological Hamiltonian comprising the Argonne v_6' (AV6P) NN potential [36] and the Urbana IX (UIX) NNN potential [37,38].

The AV6P potential is determined projecting the full Argonne v_{18} potential of Ref. [35] (AV18) onto the operator basis comprising the terms with $p \leq 6$ in the right-hand side of Eq. (3). It predicts the binding energy and electric quadrupole moment of the deuteron with accuracy of 1%, and 4%, respectively, and provides an excellent fit of the

[1]In this article, we adopt the system of natural units, in which $\hbar = c = k_B = 1$, and, unless otherwise specified, neglect the small proton-neutron mass difference.

NN scattering phase shifts in the $^1S_0$ channel—corresponding to total spin and isospin $S = 0$ and $T = 1$, and relative angular momentum $\ell = 0$—providing the dominant contribution to the energy of neutron matter. The contributions originating from states with $\ell > 0$ turn out to largely cancel among themselves; see, e.g., Ref. [39].

The UIX potential is written in the form

$$V_{ijk} = V_{ijk}^{2\pi} + V_{ijk}^{R}, \tag{4}$$

where the first term is the attractive Fujita-Miyazawa potential—describing two-pion exchange NNN interactions with excitation of a Δ resonance in the intermediate state—while V_{ijk}^R is a purely phenomenological repulsive term. The strength of $V_{ijk}^{2\pi}$ is adjusted to explain the observed ground-state energies of ^{3}He and ^{4}He, while that of the isoscalar repulsive contribution is fixed in such a way as to reproduce the saturation density of isospin symmetric matter, inferred from nuclear systematics.

Recent studies of the EOS of cold neutron matter—performed by Lovato *et al.* [40] using state-of-the-art computational techniques—show that the predictions of the somewhat simplified AV6P + UIX Hamiltonian are very close to those obtained from the full AV18 + UIX model, providing the basis of the widely employed EOS of Akmal, Pandharipande and Ravenhall [41,42].

The procedure to derive the effective interaction, thoroughly described in Refs. [21,28,43], exploits the formalism of correlated basis functions (CBF) and cluster expansion techniques to take into account the effects of strong nucleon-nucleon correlations, arising from the presence of a strong repulsive core in the NN potential. The resulting density-dependent effective potential—which can be written as in Eq. (3) with the sum in the right-hand side limited to $p \leq 6$—is well behaved, and consistently includes the contributions of NN and NNN interactions. As a consequence, it is expected to be well suited to perform perturbative calculations of nuclear matter properties in the density regime relevant to neutron stars.

B. Perturbation theory at finite temperature

At first order in the CBF effective interaction $v^{\rm eff}$, the internal energy per nucleon of nuclear matter at baryon density ϱ, temperature T can be written in the form [21]

$$\frac{E}{N} = \frac{1}{N}\left\{\sum_{\alpha\mathbf{k}} \frac{\mathbf{k}^2}{2m} n_\alpha(k,T) + \frac{1}{2}\sum_{\alpha\mathbf{k}}\sum_{\alpha'\mathbf{k}'} \langle \alpha k, \alpha' k' | v^{\rm eff} | \alpha k, \alpha' k' \rangle_A n_\alpha(k,T) n_{\alpha'}(k',T)\right\}. \tag{5}$$

In the above equation, $\mathbf{k}$ is the nucleon momentum, with $k = |\mathbf{k}|$, the index $\alpha = n, p$ labels neutrons and protons, with $Y_\alpha = \varrho_\alpha/\varrho$ being the corresponding fraction, and $|\alpha k, \alpha' k'\rangle_A$ denotes an antisymmetrized two-nucleon state. Note that conservation of baryon number requires that $Y_n = 1 - Y_p$.

The temperature dependence is described by the Fermi distribution,

$$n_\alpha(k,T) = \{1 + \exp[\beta(e_{\alpha k} - \mu_\alpha)]\}^{-1}. \tag{6}$$

where the single-particle energy is defined as

$$e_{\alpha k} = e_{\alpha k}^{\rm HF} + \delta e, \tag{7}$$

with

$$e_{\alpha k}^{\rm HF} = \frac{\mathbf{k}^2}{2m} + \sum_{\alpha'\mathbf{k}'} \langle \alpha k, \alpha' k' | v^{\rm eff} | \alpha k, \alpha' k' \rangle_A n_\alpha(k',T), \tag{8}$$

and

$$\delta e = \frac{\varrho}{2}\sum_{\alpha\mathbf{k}}\sum_{\alpha'\mathbf{k}'} \langle \alpha k, \alpha' k' | \frac{\partial v^{\rm eff}}{\partial \varrho} | \alpha k, \alpha' k' \rangle_A n_\alpha(k,T) n_{\alpha'}(k',T), \tag{9}$$

The correction to the Hartree-Fock (HF) spectrum is needed to satisfy the requirement of thermodynamic consistence, and vanishes in the case of a density-independent potential; see Ref. [21] for details.

The chemical potentials μ_α are determined by the normalization conditions,

$$\frac{2}{V}\sum_{\alpha\mathbf{k}} n_\alpha(k,T) = \varrho_\alpha, \tag{10}$$

where V is the normalization volume, and the number density of particles of species α is defined as $\varrho_\alpha = Y_\alpha \varrho$. Note that the above definitions imply that both the single-nucleon energies and the chemical potentials depend on temperature through the Fermi distribution.

The entropy per nucleon is also defined in terms of the distribution of Eq. (6) as

$$\frac{S}{N} = -\frac{1}{N}\sum_{\alpha\mathbf{k}}\{n_\alpha(k,T)\ln n_\alpha(k,T) + [1 - n_\alpha(k,T)]\ln[1 - n_\alpha(k,T)]\}. \tag{11}$$

Finally, the Helmoltz free energy per nucleon is obtained combining Eqs. (5) and (11) in the form

$$\frac{F}{N} = \frac{1}{N}(E - TS). \tag{12}$$

III. THERMAL EFFECTS

In the temperature regime considered in the present study, thermal modifications of nuclear matter properties

arise primarily from the Fermi distribution, defined by Eq. (6). Comparison to the $T \to 0$ limit

$$n_\alpha(k,0) = \theta(\mu_\alpha - e_{\alpha k}), \tag{13}$$

where $\theta(x)$ is the Heaviside theta function, shows that the probability distribution $n_\alpha(k, T > 0)$ is reduced from unity in the region corresponding to $\mu_\alpha - T \lesssim e_{\alpha k} \lesssim \mu_\alpha$, while acquiring a nonvanishing positive value for $\mu_\alpha \lesssim e_{\alpha k} \lesssim \mu_\alpha + T$. It follows that, for any given temperature T, the extent of thermal modifications to the Fermi distribution is driven by the ratio $2T/\mu_{\alpha k}$. This observation in turn implies that, because the chemical potential is a monotonically increasing function of the particle density ϱ_α, for any given T thermal effects are more significant at lower ϱ_α. On the other hand, they become vanishingly small in the high-density regime, in which degeneracy becomes dominant.

The density dependence of thermal effects—which also affects the particle energies and chemical potentials, defined by Eqs. (7) and (10), respectively—plays a significant role in the determination of the properties of multicomponent systems, such as charge-neutral β-stable matter, in which different particles have different densities.

A. Composition of charge-neutral β-stable matter

In charge-neutral matter consisting of neutrons, protons and leptons in equilibrium with respect to the weak interaction processes

$$n \to p + \ell^- + \bar{\nu}_\ell, \qquad p + \ell^- \to n + \nu_\ell, \tag{14}$$

where $\ell = e, \mu$ labels the lepton flavor, the proton fraction $Y_p = \varrho_p/\varrho$ is uniquely determined by the equations

$$\mu_n - \mu_p = \mu_\ell, \tag{15}$$

$$Y_p = \sum_\ell Y_\ell. \tag{16}$$

Note that Eq. (15) is obtained under the assumption that matter is transparent to the produced neutrinos, implying on turn that neutrinos have vanishing density and chemical potential. At densities such that the electron chemical potential does not exceed the rest mass of the muon, $m_\mu = 105.7$ MeV, the sum appearing in the above equation includes electrons only. However, at higher densities—typically at $\varrho \gtrsim \varrho_0$, with $\varrho_0 = 0.16$ fm^{-3} being the equilibrium density of isospin-symmetric matter—the appearance of muons becomes energetically favored, and must be taken into account.

The solid lines of Fig. 1 show the density dependence of the proton fractions corresponding to β equilibrium of matter consisting of protons, neutrons, electrons and muons, or $npe\mu$ matter, at $T = 0$ (triangles) and 50 MeV (circles); all results have been obtained using the formalism described in Ref. [21]. For comparison, the same quantities in npe matter, in which the muon contribution is not included, are displayed by the dashed lines.

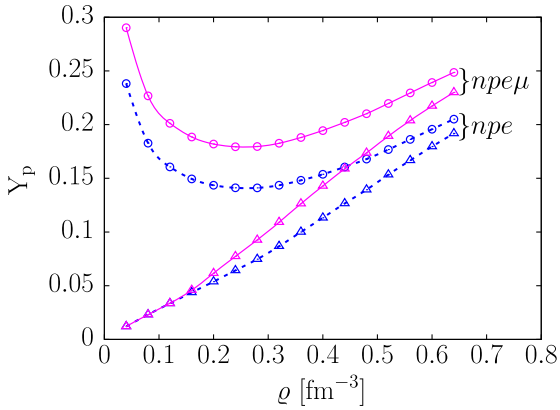

FIG. 1. Density dependence of the proton fraction in charge-neutral β-stable matter. Solid lines marked with triangles and circles correspond to $npe\mu$ matter at $T = 0$ and 50 MeV, respectively. The same quantities in npe matter are represented by dashed lines.

The most prominent thermal effect is a significant departure from the monotonic behavior observed in cold matter. The emergence of a minimum in the density dependence of the proton fraction results from the interplay between the thermal and degeneracy contributions to the chemical potentials appearing in Eq. (15). For $T \gtrsim 20$ MeV and low density, typically $\varrho \lesssim \varrho_0$, the thermal contribution —whose leading order term can be written in the form $\delta\mu_\alpha \propto T^2/\varrho_\alpha^{2/3}$—turns out to be much larger for protons than for neutrons, and β equilibrium requires large proton fractions.

B. Fermi distributions

The Fermi distribution of Eq. (6) depends on temperature both explicitly, through the factor $\beta = 1/T$ appearing in the argument of the exponential, and implicitly, through the T dependence of both $e_{\alpha k}$ and μ_α. Because the calculation of single-particle energies and chemical potentials in turn involves the Fermi distribution, $e_{\alpha k}$, μ_α and $n_\alpha(k,T)$ must, in fact, be determined self-consistently, applying an iterative procedure.

Figure 2 shows the distributions of neutrons and protons in charge-neutral β-stable $npe\mu$ matter at baryon density $\varrho = 0.32$ fm^{-3}.

It is apparent that, as pointed out in the previous section, thermal modifications to $n_\alpha(k,T)$—extending over a region of width $2T$ around the Fermi momentum $k_{F\alpha} = (3\pi^2\varrho_\alpha)^{1/3}$—depend on *both* temperature *and* density. As a consequence, for any given temperature T they are more pronounced in the case of protons, whose density is suppressed by a factor $Y_p/(1 - Y_p) \ll 1$ with respect to the neutron density.

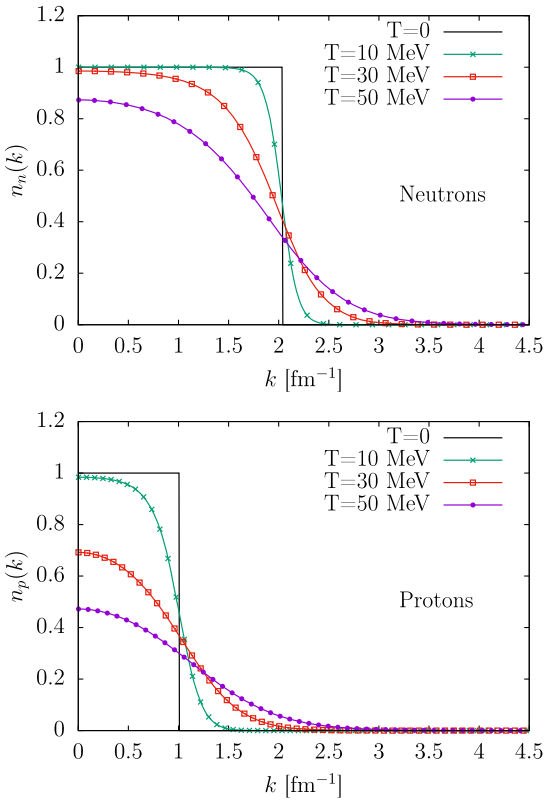

FIG. 2. Neutron and proton Fermi distributions in charge-neutral β-stable $npe\mu$ matter at baryon density $\varrho = 0.32$ fm^{-3}.

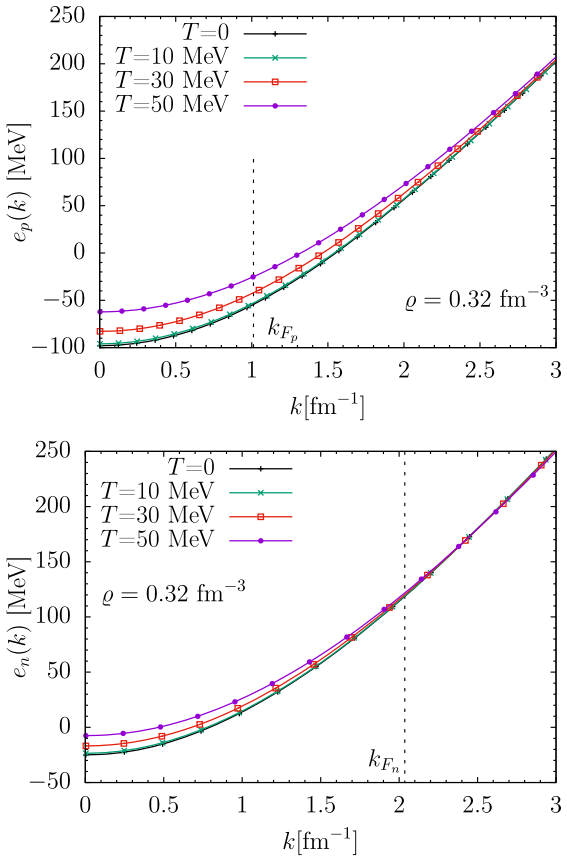

FIG. 3. Neutron and proton spectra in β-stable $npe\mu$ matter at baryon density $\rho = 0.32$ fm^{-3}, and temperatures in the range $0 \le T \le 50$ MeV.

C. Nucleon energy spectra and effective masses

The proton and neutron spectra employed to calculate the Fermi distributions of Fig. 2—corresponding to β-stable $npe\mu$ matter at baryon density $\varrho = 2\varrho_0$—are displayed in Fig. 3. It is apparent that $e_{\alpha k}$ is an increasing function of temperature at all values of k, with the T dependence being stronger at lower momentum. At $k = 0$ the difference between the energies corresponding to $T = 0$ and 50 MeV reaches ∼35.8 MeV for protons, and ∼17.5 MeV for neutrons. In the case of protons, a ∼29 MeV increase with respect to the zero-temperature spectrum is still clearly visible at $k = k_{F_p}$, $k_{F_p} = 1.01$ fm^{-1} being the proton Fermi momentum, while the $T = 0$ and 50 MeV neutron spectra at $k = k_{F_n}$, with $k_{F_n} = 2.04$ fm^{-1}, are nearly indistinguishable.

As an illustration of the overall decrease of thermal effects with increasing baryon density, Fig. 4 shows the proton and neutron spectra in β-stable $npe\mu$ matter at $\varrho = 0.48$ fm^{-3}.

In theoretical calculations of nuclear matter properties of astrophysical interest—such as the neutrino emission rates [4], and the shear and bulk viscosity coefficients [10,44,45]—the relevant information comprised in proton and neutron spectra is captured by the corresponding effective masses $m^\star_\alpha$, defined by the equations

$$\frac{1}{m^\star_\alpha} = \left(\frac{1}{k}\frac{de_{\alpha k}}{dk}\right)_{k=k_{F_\alpha}}. \tag{17}$$

The role played by the effective masses can be readily grasped considering that they determine the dispersion relations of matter constituents, which in turn affect their collision rates through both the incident flux and the available phase space.

The density dependence of the proton and neutron effective masses of charge-neutral β-stable $npe\mu$ matter at temperature $0 \le T \le 50$ MeV is illustrated in Fig. 5. It clearly appears that, regardless of temperature, $m^\star_\alpha$ is a monotonically decreasing function of baryon density. For neutrons, thermal effects—measured by the departure from the zero-temperature effective mass—turn out to be limited to ∼5% over the whole temperature and density range considered. For protons, on the other hand, their size for $T = 50$ MeV turns out to be ∼25% at $\varrho = \varrho_0$, and is still $\gtrsim$10% at $\varrho = 4\varrho_0$.

The nucleon effective masses are routinely used to parametrize the momentum dependence of the nucleon spectra in cold nuclear matter according to [4]

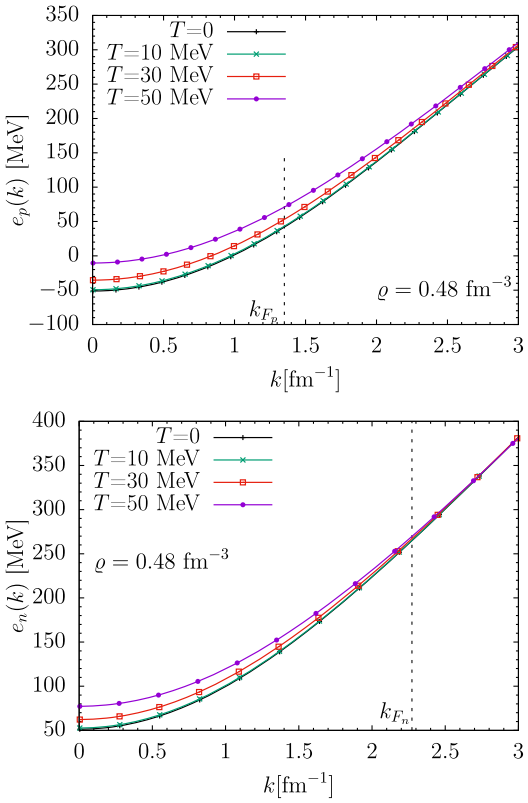

FIG. 4. Same as in Fig. 3, but for matter at baryon density $\varrho = 0.48$ fm^{-3}.

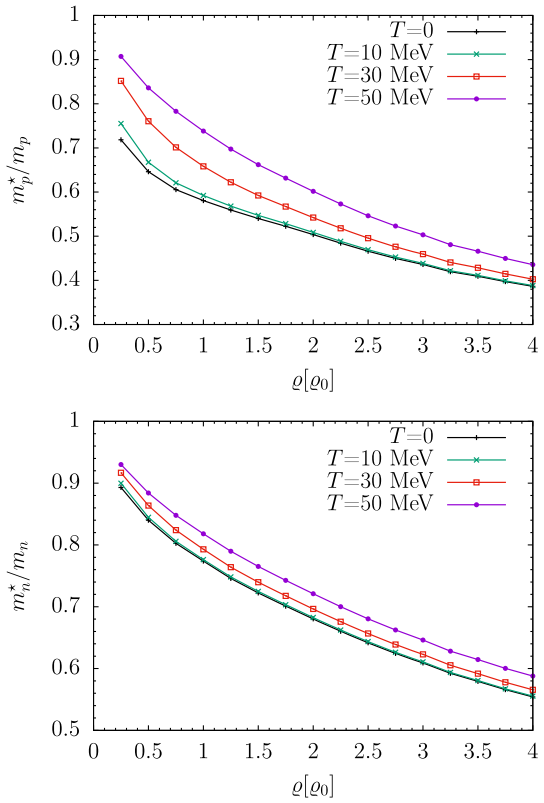

FIG. 5. Density dependence of the proton and neutron effective masses of charge-neutral β-stable matter at temperature $0 \le T \le 50$ MeV. Baryon densities are measured in units of the equilibrium density of cold isospin-symmetric matter.

$$e_{\alpha k} = \frac{k^2}{2m_0^\star} + U_\alpha, \tag{18}$$

where $m_0^\star$ denotes the value of $m_\alpha^\star$ at $T = 0$, while the offset U_α is determined by the requirement that the above approximation reproduce the spectrum obtained from the full microscopic calculation in the $k \to 0$ limit.

In Fig. 6 the proton spectra in β-stable $npe\mu$ matter at baryon density $\varrho_B = 0.32$ fm^{-3} and temperature $T = 0$ and 50 MeV, obtained from Eqs. (7)–(9), are compared to those computed using Eq. (18). At $T = 0$ the quadratic approximation turns out to be remarkably accurate up to momenta largely above the Fermi momentum, $k_{F_p} = 1.01$ fm^{-1}. At $T = 50$ MeV, on the other hand, the agreement between the results of the two calculations is somewhat degraded; the discrepancy is ∼25% at $k = k_{F_p}$, and monotonically increases with k.

The spectra displayed in the bottom panel of Fig. 6 clearly show that the accuracy of Eq. (6) at $T > 0$ can be significantly improved by taking into account the temperature dependence of the effective mass, which amounts to replacing $m_0^\star$ with the appropriate finite-temperature value, obtained from Eq. (17).

In the literature, the temperature dependence of $e_{\alpha k}$ is often disregarded, and the properties of nuclear matter at $T > 0$ are calculated using zero-temperature spectra. This approximation, referred to as *frozen correlations approximation* (FCA), has been recently employed in the studies of binary neutron star mergers of Figura *et al.* [7,8]. The results reported in Ref. [46] suggest that the FCA has a nearly negligible effect on the thermodynamic properties of nuclear matter at $T \lesssim 30$ MeV. However, its accuracy has been shown to deteriorate at larger temperatures [47]. The validity of the assumption underlying the FCA can be gauged from Figs. 3 and 4. The implications of using this approximation scheme in calculations of nuclear matter properties will be discussed further in the next section.

D. Chemical potentials and matter composition

Within the theoretical approach underlying our work, thoroughly discussed in Ref. [21], thermodynamic consistency is satisfied by construction. To illustrate this property, in Fig. 7 the chemical potential defined in Eq. (10) is compared to the one obtained from the thermodynamic definition,

$$\mu_\alpha = \left(\frac{\partial F}{\partial N_\alpha}\right)_{V, N_{\alpha' \neq \alpha}}, \tag{19}$$

using the free energy of Eq. (12).

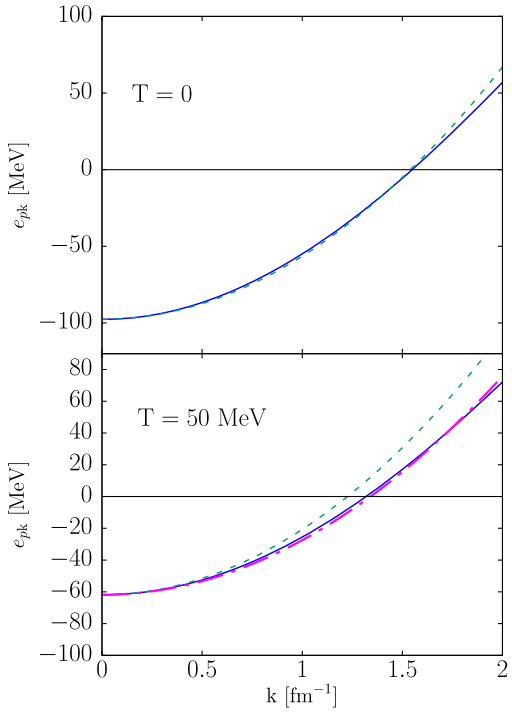

FIG. 6. Proton spectra in charge-neutral, β-stable matter at $T = 0$ (upper panel) and 50 MeV (lower panel). The solid lines represent results of calculations carried out using Eqs. (7)–(9), while the dashed lines have been obtained from the quadratic approximation of Eq. (18) with the zero-temperature effective mass. The dot-dashed line in the lower panel illustrates the effect of the thermal dependence of $m_p^\star$; see text for details.

The chemical potentials of protons and neutrons in charge-neutral β-stable matter at temperature $T = 0$ and 50 MeV are displayed in Fig. 8 as a function of baryon density. For comparison, the difference $\mu_n - \mu_p = \mu_e$ is also shown.

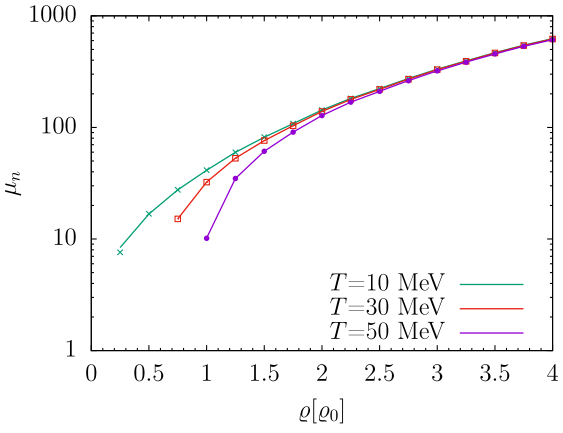

FIG. 7. Comparison between the neutron chemical potential in pure neutron matter computed using Eq. (10), represented by the solid lines, and that obtained from the thermodynamic definition using the free energy of Eq. (12).

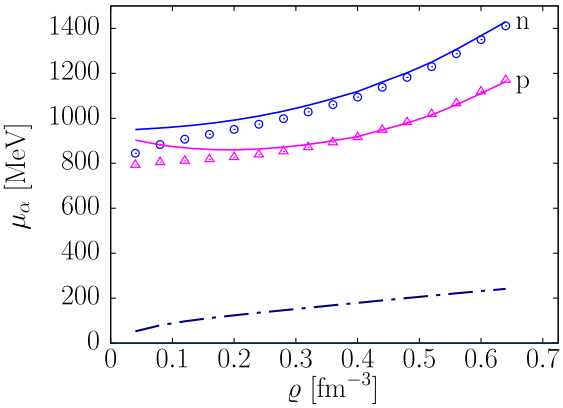

FIG. 8. Density dependence of the chemical potentials of protons (p) and neutrons (n) in β-stable matter ar $T = 50$ MeV. For comparison, the corresponding quantities at $T = 0$ are shown by the solid lines. The dot-dashed line represents the difference $\mu_n - \mu_p$ at $T = 50$ MeV.

Thermal effects on chemical potentials can be analyzed considering the difference,

$$\delta\mu_{\alpha,\mathrm{th}} = \mu_\alpha - \mu_{\alpha,0}, \tag{20}$$

with $\mu_{\alpha,0}$ being the value of μ_α in cold matter at fixed baryon density ϱ_B and particle fraction Y_α. Figure 9 illustrates the temperature dependence of $\delta\mu_{n,\mathrm{th}}$ in charge-neutral β-stable matter at baryon density $\varrho = 2\varrho_0$.

Because thermal effects in β-stable matter have a different impact on proton and neutron properties, the capability to accurately predict β equilibrium and matter composition using FCA must be carefully investigated. The results of numerical calculations carried out within our approach indicate for temperatures up to $T = 50$ MeV the discrepancy between the proton fractions obtained from FCA and the exact results never exceeds ~3% over the considered range of baryon density.

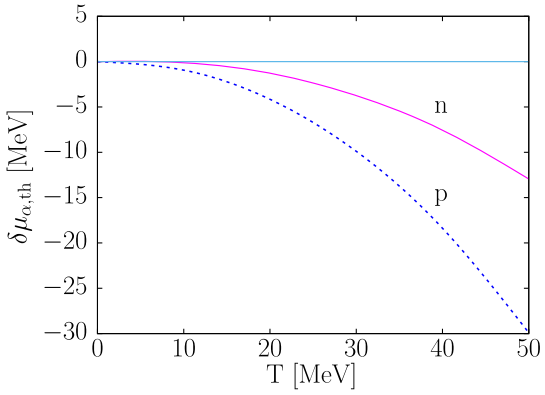

FIG. 9. Temperature dependence of the thermal contribution to the proton (p) and neutron (n) chemical potentials, defined by Eq. (20), in β-stable matter at baryon density $\varrho_B = 2\varrho_0$.

TABLE I. Properties of isospin-symmetric matter at $T = 0$ obtained by the authors or Ref. [28] using the CBF effective interaction described in this article. The experimental values of the compressibility module, K_0, and symmetry energy, $E_{\rm sym}(\rho_0)$, are taken from Refs. [48,49] and [50], respectively.

	ρ_0 [fm^{-3}]	$E(\rho_0)/N$ [MeV]	K_0 [MeV]	$E_{\rm sym}(\rho_0)$ [MeV]
Ref. [28]	0.16	−11.0	210.0	30.9
Experiment	0.16	−16.0	240.0 ± 20.0	31.6 ± 2.66

E. Internal energy and free energy

The results of a detailed study of the properties of cold nuclear matter—performed by the authors of Ref. [28] using the CBF effective interaction discussed in this article—are collected in Table I. This analysis shows that the AV6P + UIX Hamiltonian reproduces the correct equilibrium density of isospin-symmetric matter, and yields values of the compressibility module and symmetry energy largely compatible with the available data. As for the energy per nucleon, it should be kept in mind that, because kinetic and interaction energies largely cancel one another, the 5 MeV discrepancy in the value of $E(\rho_0)/N$ translates into a ∼15% underestimate of the empirical interaction energy. This result is within ∼7% of that reported by Akmal *et al.* [42], who performed an accurate variational calculation of symmetric nuclear matter with the full AV18 + UIX Hamiltonian.

The density and temperature dependence of the internal energy and entropy per baryon of β-stable matter, defined according to Eqs. (5) and (11), respectively, is illustrated in Figs. 10 and 11.

Figure 10 shows that, for any given ϱ, the internal energy is an increasing function of temperature. However, the concurrent increment of the proton fraction with T, discussed in Sec. III A, leads to the appearance of a minimum for temperatures larger than 10 MeV.

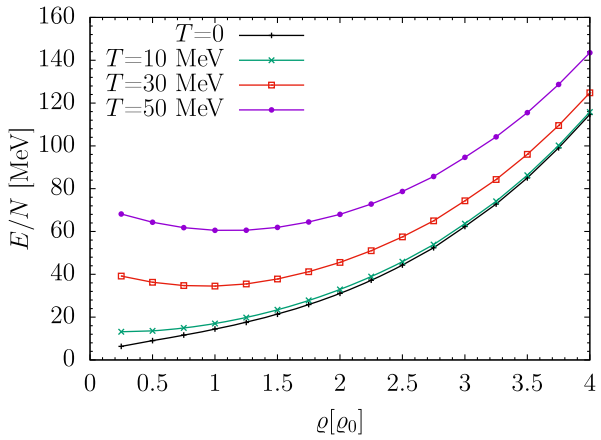

FIG. 10. Internal energy per baryon of beta-stable matter as a function of baryon density for different temperatures. Note that ϱ is given in units of the equilibrium density of cold isospin-symmetric matter, $\varrho_0 = 0.16$ fm^{-3}.

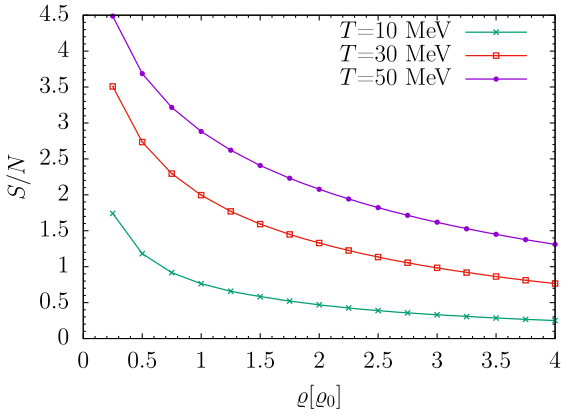

FIG. 11. Entropy per baryon of beta-stable matter as a function of density for different temperatures. Note that ϱ is given in units of the equilibrium density of cold isospin-symmetric matter, $\varrho_0 = 0.16$ fm^{-3}.

As expected, thermal contributions to the internal energy turn out to be less important at higher ϱ. However, for $T >$ 10 MeV they are still significant at densities as high as $4\varrho_0$.

IV. MODELING THERMAL EFFECTS

The description of thermal effects on the thermodynamic functions determining the EOS, that is, pressure and energy density, is of paramount importance in view of astrophysical applications. The number of available EOSs of nuclear matter at $T \neq 0$ is much smaller when compared to the corresponding figure for cold matter. Moreover, the implementation of microscopic EOSs in numerical simulation of processes such as binary neutron star merger involves nontrivial difficulties [51,52].

These above problems are often circumvented using simple but physically sound parametrization of the EOSs. An extensively used expression is based on the so-called hybrid-EOS approach, in which thermal contributions to pressure and energy density are described using an approximation based on the ideal fluid law; see Eq. (1).

As pointed out in the previous section, the results of microscopic calculations clearly signal a strong interplay between the dependencies of the nuclear matter properties on density and temperature. This feature obviously questions the adequacy of the assumption that thermal contributions to the EOS be the same to all densities. Motivated by this observation, Raithel *et al.* have recently proposed a model that explicitly takes into consideration the effect of matter degeneracy [16].

Rather than using the ideal fluid EOS in the whole density range, the authors of Ref. [16] employ the Sommerfeld expansion described by Constantinou *et al.* [53] in the region high ϱ. This formalism allows to write the deviations of the thermodynamic functions from their zero-

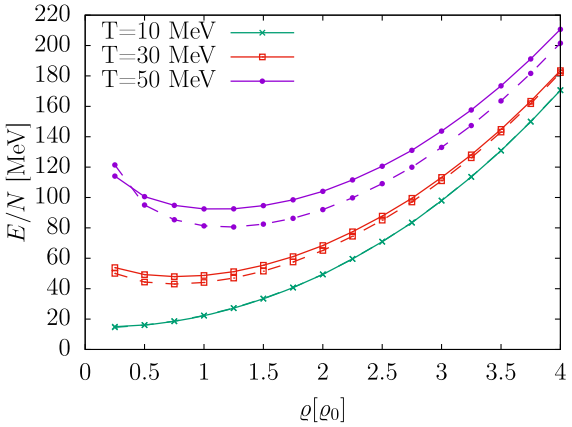

FIG. 12. Density dependence of the internal energy per baryon of npe matter in β equilibrium. Solid and dashed lines correspond to the results of our calculations and to the fit of Refs. [16,54].

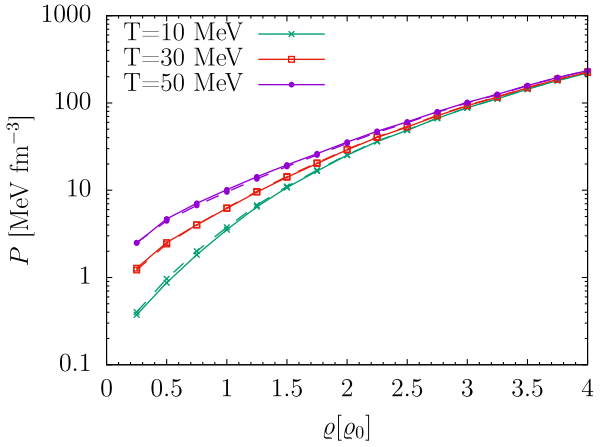

FIG. 13. Comparison between the pressure of β-stable npe matter obtained using the approximate model of Refs. [16,54] (dashed lines) and the microscopic approach described in this work (solid lines).

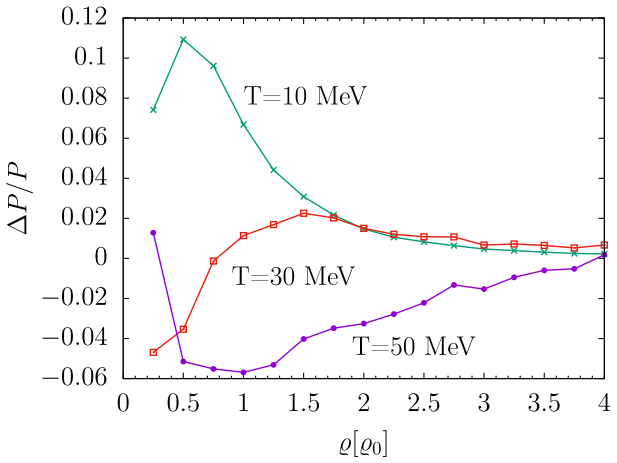

FIG. 14. Relative difference between the pressure of β-stable npe matter obtained using the model of Raithel *et al.* [6] and that resulting from the microscopic approach described in this work.

temperature values as series of powers of T. The calculation of the next-to-leading order term involves the nucleon effective mass and its derivatives, which implies that a model of nuclear dynamics at $T \neq 0$ is needed beforehand.

In order to make their parametrization as general as possible, Raithel *et al.* [16] considered a set of RMF models for which the effective masses at different temperatures are available in the literature, and performed a fit using analytical models, such as piecewise polytropes, as zero-temperature baseline.

Our goal here is establish the extent to which the results reported in Ref. [16] stand, when compared to an EOS obtained within the framework of NMBT, rather than the RMF approach. We use the parameter values $n_0 \sim 0.13$ fm^{-3} and $\alpha \sim 0.9$—see box 1 of Ref. [16] and the erratum, Ref. [54]—to obtain first the effective mass, and subsequently the internal energy per baryon and the matter pressure. Note that the results reported in Ref. [16] do not include the contribution of muons. Therefore, our analysis will be limited to the case of npe matter.

In Fig. 12 we show a comparison between the internal energy per baryon of β-stable npe matter obtained from the approach described in the previous section (solid lines) and the fit of Refs. [16,54] (dashed lines). It is apparent that at $T = 10$ MeV, the agreement is almost perfect, while discrepancies—the size of which increases with increasing T—are clearly visible at larger temperatures. The maximum relative error between the fit and the microscopic calculation at $T = 50$ MeV (30 MeV) turns out to be $\sim$16% ($\sim$11%), and occurs at density $\sim 1.5\varrho_0$ ($\sim\varrho_0$).

We have also analyzed the accuracy of the approximation of Raithel *et al.* [16] for the pressure. A comparison with the results obtained from our microscopic approach, illustrated in Fig. 13, shows a remarkably good agreement over the whole temperature range. The parametrization of Ref. [16] appears to properly take into account the effects of degeneracy at all densities.

In order to provide a quantitative estimate of the validity of the approximations involved in the parametrization of pressure, in Fig. 14 we report the relative difference,

$$\frac{\Delta P}{P} = \frac{(P_{\text{approx}} - P)}{P}, \tag{21}$$

where P is the result of our calculation, as a function of baryon density. It is apparent that for $T = 10$ MeV the error is always less than $\sim$3%, and never exceeds $\sim$13% for temperatures up to 50 MeV.

V. SUMMARY AND CONCLUSIONS

We have analyzed the impact of temperature on several properties of charge-neutral nuclear matter in β equilibrium. Calculations have been performed using the

formalism of finite-temperature perturbation theory, with an effective interaction derived from a nuclear Hamiltonian comprising both two- and three-nucleon potentials.

The most prominent feature emerging from our results is the strong interplay between temperature and density, which can be ultimately traced back to the form of the Fermi distribution. For any given temperature thermal effects turn out to decrease with density, although in some instances they are still significant at density as high as $\sim 4\varrho$. As a consequence, in β-stable matter thermal modifications of nucleon properties, such as the energy spectrum, are more pronounced for protons than for neutrons.

The interplay of temperature and density has no trivial implications for astrophysical studies. The temperature and density profiles obtained from neutron star merger simulations—see, e.g., Refs. [6,7,55]—show that in the inner region of the remnant the thermal contribution to the pressure is lower. However, this happens not only because the degeneracy pressure becomes more important, but also because the temperature is lower. On the other hand, at intermediate densities the temperature is higher and the thermal contribution to the pressure is larger as well. At lower densities, despite the temperature being lower, the thermal contribution to the pressure is even more important due to naturally lower degeneracy pressure. It clearly appears that, in order to pin down the role of thermal effects in determining the properties of neutron star matter, their temperature and density dependence must be accurately described within a consistent framework.

Of great importance, in this context, will be the availability of simple parametrizations of the EOS of hot nuclear matter in β equilibrium, suitable for use in numerical simulations. A direct comparison to the results of our calculations shows that the approximate treatment of thermal effects recently proposed by Raithel *et al.* [6] is remarkably accurate, and suitable to describe EOSs obtained from different models of nuclear dynamics.

It is important to keep in mind that the discussion of temperature effects in nuclear matter should not be limited to thermal contributions to average properties, such as the pressure and energy density. As shown by the results discussed in this article, the most fundamental properties, including the Fermi distributions, single-particle spectra and effective masses, are significantly modified at finite temperature. A consistent inclusion of the temperature dependence of these quantities is essential to accurately describe nuclear collision rates in matter, which in turn determine out-of-equilibrium phenomena [10,45,56,57], as well as neutrino emission. The approach described in this article allows to carry out calculations of, e.g., the rates of modified Urca processes at $T > 0$, using nuclear matrix elements obtained from a highly realistic nuclear Hamiltonian, comprising both two- and three-nucleon potentials.

As a final remark, is should be also mentioned that in this work we have considered β equilibrium in the absence of neutrinos. However, neutrino trapping is expected to occur even at $T \lesssim 10$ MeV [58], and we plan to extend our calculations to study this scenario.

ACKNOWLEDGMENTS

This work has been supported by the Italian National Institute for Nuclear Research (INFN) under Grant TEONGRAV. O. B. gratefully acknowledges the kind hospitality of the Center for Neutrino Physics at Virginia Tech, where part of this work has been carried out.

[1] A. Burrows and J. M. Lattimer, Astrophys. J. **307**, 178 (1986).
[2] W. Keil and H. T. Janka, Astron. Astrophys. **296**, 145 (1995), https://ui.adsabs.harvard.edu/abs/1995A%26A...296..145K/abstract.
[3] J. A. Pons, S. Reddy, M. Prakash, J. M. Lattimer, and J. A. Miralles, Astrophys. J. **513**, 780 (1999).
[4] G. Camelio, A. Lovato, L. Gualtieri, O. Benhar, J. A. Pons, and V. Ferrari, Phys. Rev. D **96**, 043015 (2017).
[5] L. Baiotti and L. Rezzolla, Rep. Prog. Phys. **80**, 096901 (2017).
[6] C. A. Raithel, V. Paschalidis, and F. Özel, Phys. Rev. D **104**, 063016 (2021).
[7] A. Figura, J.-J. Lu, G. F. Burgio, Z.-H. Li, and H.-J. Schulze, Phys. Rev. D **102**, 043006 (2020).
[8] A. Figura, F. Li, J.-J. Lu, G. F. Burgio, Z.-H. Li, and H.-J. Schulze, Phys. Rev. D **103**, 083012 (2021).
[9] P. Hammond, I. Hawke, and N. Andersson, Phys. Rev. D **104**, 103006 (2021).
[10] M. G. Alford, L. Bovard, M. Hanauske, L. Rezzolla, and K. Schwenzer, Phys. Rev. Lett. **120**, 041101 (2018).
[11] A. Perego, S. Bernizzi, and D. Radice, Eur. Phys. J. A **55**, 124 (2019).
[12] A. Endrizzi, A. Perego, F. M. Fabbri, L. Branca, D. Radice, S. Bernuzzi, B. Giacomazzo, F. Pederiva, and A. Lovato, Eur. Phys. J. A **56**, 15 (2020).
[13] M. Cusinato, F. M. Guercilena, A. Perego, D. Logoteta, D. Radice, S. Bernuzzi, and S. Ansoldi, Eur. Phys. J. A **58**, 99 (2022).
[14] I. Vidaña, D. Logoteta, and I. Bombaci, Phys. Rev. C **106**, 035804 (2022).
[15] CompOSE: CompStar Online Supernovæ Equations of State, https://compose.obspm.fr/articles.

[16] C. A. Raithel, F. Özel, and V. Paschalidis, Astrophys. J. **875**, 12 (2019).
[17] R. Oechslin, H.-T. Janka, and A. Marek, Astron. Astrophys. **467**, 395 (2007).
[18] M. Prakash, I. Bombaci, M. Prakash, P. J. Ellis, J. M. Lattimer, and R. Knorren, Phys. Rep. **280**, 1 (1997).
[19] J. D. Kaplan, C. D. Ott, E. P. O'Connor, K. Kiuchi, L. Roberts, and M. Duez, Astrophys. J. **790**, 19 (2014).
[20] J.-J. Lu, Z.-H. Li, G. F. Burgio, A. Figura, and H.-J. Schulze, Phys. Rev. C **100**, 054335 (2019).
[21] O. Benhar, A. Lovato, and G. Camelio, Astrophys. J. **939**, 52 (2022).
[22] C. Wellenhofer, J. W. Holt, N. Kaiser, and W. Weise, Phys. Rev. C **89**, 064009 (2014).
[23] A. Carbone and A. Schwenk, Phys. Rev. C **100**, 025805 (2019).
[24] J. Keller, C. Wellenhofer, K. Hebeler, and A. Schwenk, Phys. Rev. C **103**, 055806 (2021).
[25] D. Logoteta, A. Perego, and I. Bombaci, Astron. Astrophys. **646**, A55 (2021).
[26] I. Tews, J. Carlson, S. Gandolfi, and S. Reddy, Astrophys. J. **860**, 149 (2018).
[27] O. Benhar, Int. J. Mod. Phys. E **30**, 2130009 (2021).
[28] O. Benhar and A. Lovato, Phys. Rev. C **88**, 064005 (2013).
[29] A. Bauswein, H.-T. Janka, and R. Oechslin, Phys. Rev. D **82**, 084043 (2010).
[30] K. Hotokezaka, K. Kyutoku, H. Okawa, M. Shibata, and K. Kiuchi, Phys. Rev. D **83**, 124008 (2011).
[31] A. Endrizzi, R. Ciolfi, B. Giacomazzo, W. Kastaun, and T. Kawamura, Classical Quantum Gravity **33**, 164001 (2016).
[32] T. Dietrich, S. Bernuzzi, M. Ujevic, and W. Tichy, Phys. Rev. D **95**, 044045 (2017).
[33] T. Dietrich, M. Ujevic, W. Tichy, S. Bernuzzi, and B. Brügmann, Phys. Rev. D **95**, 024029 (2017).
[34] C. Constantinou, B. Muccioli, M. Prakash, and J. M. Lattimer, Ann. Phys. (Amsterdam) **363**, 533 (2015).
[35] R. B. Wiringa, V. G. J. Stoks, and R. Schiavilla, Phys. Rev. C **51**, 38 (1995).
[36] R. B. Wiringa and S. C. Pieper, Phys. Rev. Lett. **89**, 182501 (2002).
[37] B. S. Pudliner, V. R. Pandharipande, J. Carlson, and R. B. Wiringa, Phys. Rev. Lett. **74**, 4396 (1995).
[38] J. Carlson, V. R. Pandharipande, and R. B. Wiringa, Nucl. Phys. **A401**, 59 (1983).
[39] M. Kohno, Phys. Rev. C **88**, 064005 (2013).
[40] A. Lovato, I. Bombaci, D. Logoteta, M. Piarulli, and R. B. Wiringa, Phys. Rev. C **105**, 055808 (2022).
[41] A. Akmal and V. R. Pandharipande, Phys. Rev. C **56**, 2261 (1997).
[42] A. Akmal, V. R. Pandharipande, and D. G. Ravenhall, Phys. Rev. C **58**, 1804 (1998).
[43] A. Lovato, C. Losa, and O. Benhar, Nucl. Phys. **A901**, 22 (2013).
[44] O. Benhar and M. Valli, Phys. Rev. Lett. **99**, 232501 (2007).
[45] M. Alford, A. Harutyunyan, and A. Sedrakian, Phys. Rev. D **104**, 103027 (2021).
[46] M. Baldo and L. S. Ferreira, Phys. Rev. C **59**, 682 (1999).
[47] G. F. Burgio and H.-J. Schulze, Astron. Astrophys. **518**, A10 (2010).
[48] S. Shlomo, V. M. Kolomietz, and G. Colò, Eur. Phys. J. A **30**, 23 (2006).
[49] G. Colò, Phys. Part. Nucl. **39**, 286 (2008).
[50] B.-A. Li and X. Han, Phys. Lett. B **727**, 276 (2013).
[51] S. Bernuzzi *et al.*, Mon. Not. R. Astron. Soc. **497**, 1488 (2020).
[52] V. Nedora, S. Bernuzzi, D. Radice, B. Daszuta, A. Endrizzi, A. Perego, A. Prakash, M. Safarzadeh, F. Schianchi, and D. Logoteta, Astrophys. J. **906**, 98 (2021).
[53] C. Constantinou, B. Muccioli, M. Prakash, and J. M. Lattimer, Ann. Phys. (Amsterdam) **363**, 533 (2015).
[54] C. A. Raithel, F. Özel, and D. Psaltis, Astrophys. J. **915**, 73 (2021).
[55] G. Camelio, T. Dietrich, S. Rosswog, and B. Haskell, Phys. Rev. D **103**, 063014 (2021).
[56] E. R. Most, S. P. Harris, C. Plumberg, M. G. Alford, J. Noronha, J. Noronha-Hostler, F. Pretorius, H. Witek, and N. Yunes, Mon. Not. R. Astron. Soc. **509**, 1096 (2021).
[57] E. R. Most, A. Haber, S. P. Harris, Z. Zhang, M. G. Alford, and J. Noronha, arXiv:2207.00442.
[58] M. G. Alford and S. P. Harris, Phys. Rev. C **98**, 065806 (2018).